A stochastic analysis of transient two-phase flow in heterogeneous porous media

Mingjie Chen,[1,2] Arturo A. Keller,[1] Dongxiao Zhang,[3] Zhiming Lu,[4] and George A. Zyvoloski[4]

Received 13 May 2005; revised 26 October 2005; accepted 18 November 2005; published 25 March 2006.

[1] The Karhunen-Loeve moment equation (KLME) approach is implemented to model stochastic transient water-NAPL two-phase flow in heterogeneous subsurface media with random soil properties. To describe the constitutive relationships between water saturation, capillary pressure, and phase relative permeability, the widely used van Genuchten model and Parker and Lenhard models are adopted. The log-transformed intrinsic permeability, soil pore size distribution, and van Genuchten fitting parameter n are treated as normally distributed stochastic variables with a separable exponential covariance model. The perturbation part of these three log-transformed variables is decomposed via Karhunen-Loeve expansion. The dependent variables (phase pressure, phase mobility, and capillary pressure) are expanded by polynomial expansions and the perturbation method. Incorporating these expansions of random soil properties variables and dependent variables into the governing equations yields a series of differential equations in different orders. We construct the moments of the dependent variables from the solutions of these differential equations. We demonstrate the stochastic model with two-dimensional examples of transient two-phase flow. We also conduct Monte Carlo simulations using the finite element heat and mass (FEHM) transfer code, whose results are considered ''true'' solutions. The match between the results from FEHM and KLME indicates the validity of the proposed KLME application in transient two-phase flow. The computational efficiency of the KLME approach over Monte Carlo methods is at least an order of magnitude for transient two-phase flow problems.

Citation: Chen, M., A. A. Keller, D. Zhang, Z. Lu, and G. A. Zyvoloski (2006), A stochastic analysis of transient two-phase flow in heterogeneous porous media, *Water Resour. Res.*, *42*, W03425, doi:10.1029/2005WR004257.

1. Introduction

[2] Groundwater contamination problems due to accidental releases of nonaqueous phase liquids (NAPL), such as organic solvents or hydrocarbon fuels, are a continuing concern. NAPL spills during transport and leaks from underground tanks and their associated piping occur frequently enough to represent a significant pollution issue and pose a potential major risk to water supply, since a small amount of NAPL can contaminate large volumes of groundwater. Moreover, NAPLs trapped in the porous soil at residual saturation are a continuous source of pollution to the subsurface aquifer.

[3] Remediation of NAPL-contaminated groundwater requires the understanding of the physicochemical processes that control the migration of NAPLs in the natural subsurface formation. Several NAPL spill models have been investigated by *Abriola* [1989], *Mercer and Cohen* [1990], *Delshad et al.* [1996], and *Keller et al.* [2000]. The organic phase can move advectively as a liquid phase, separate from the gaseous or aqueous phase. The NAPL components can also dissolve in water and be transported as solutes, or volatilize into the gas phase. It is recognized that soil heterogeneity play an important role in spill migration, as well as in the transfer of NAPL mass to the surrounding phases [e.g., *Parker et al.*, 1994]. If the soil properties are treated as random space functions, the equations governing multiphase flow in these heterogeneous formations can be treated as stochastic.

[4] The traditional method for solving these stochastic flow equations is Monte Carlo simulation [e.g., *Smith and Freeze*, 1979; *Graham and McLaughlin*, 1989; *Chin and Wang*, 1992]. It entails generation of a large number of random realizations of input variables, solving deterministic flow simulations for each realization, and calculating the moments of the dependent variables based on the results from all the realizations. This approach is conceptually straightforward, but requires intensive computational efforts since the number of realizations needed to describe the flow moments is very large in general, particularly for realistic complex sites. In addition, solving high space-time fluctuations in a random field requires a high-resolution grid and many iterations for the solution to converge, which

[1]Bren School of Environmental Sciences and Management, University of California, Santa Barbara, California, USA.
[2]Now at Hydrology, Geochemistry, and Geology Group (EES-6), Los Alamos National Laboratory, Los Alamos, New Mexico, USA.
[3]Mewbourne School of Petroleum and Geological Engineering, University of Oklahoma, Norman, Oklahoma, USA.
[4]Hydrology, Geochemistry, and Geology Group (EES-6), Los Alamos National Laboratory, Los Alamos, New Mexico, USA.

0043-1397/06/2005WR004257$09.00

demands more CPU time for each realization [e.g., *Bellin et al.*, 1992]. Convergence of the Monte Carlo method may also require increasing realization with increasing simulation time [*Tartakovsky et al.*, 2004].

[5] Compared to the Monte Carlo approach, direct stochastic analysis provides a more comprehensive and efficient method, which allows direct calculation of different statistical moments of the output variables (e.g., phase saturation, phase pressure) without generating a large number of realizations of these variables. In the last two decades, direct stochastic approaches to flow and mass transport system have been extensively studied and developed, as presented by *Dagan* [1989], *Gelhar* [1993], and *Zhang* [2002]. These approaches typically formulate moment equations with the aid of the perturbation method and spectral representation techniques. Analytical solutions of these differential equations are always desirable and more accurate than numerical solutions, though they are only available for specific cases. For example, *Chrysikopoulos et al.* [1990] and *Chrysikopoulos and Sim* [1996] presented the derivation of closed form analytical solutions of stochastic partial differential equations describing the transport of contaminants in porous media using small perturbation techniques. Most of the direct stochastic approaches have been applied to solve steady or transient saturated flow, or unsaturated flow of the water phase only.

[6] In the case of stochastic multiphase flow, few studies have been conducted, both due to the nonlinearity of the governing equations and their interdependence. One of the first studies that evaluated the mean and variance of the dependent variables such as phase and capillary pressures utilizing a direct methodology was presented by *Chang et al.* [1995]. This study presented a spectral/perturbation approach to analyze the stochastic behavior of water-oil two-phase flow in saturated porous media, whose heterogeneity was represented by the intrinsic permeability, and soil pore size distribution. *Abdin and Kaluarachchi* [1997a, 1997b] extended Chang's work to three-phase flow. *Ghanem and Dham* [1998] utilized Karhunen-Loeve decomposition techniques and polynomial chaos expansion to the stochastic analysis of two-phase flow in heterogeneous formations.

[7] The conventional moment equations (CME) method, proposed, for example, by *Graham and McLaughlin* [1989], *Zhang* [1998, 1999], *Zhang and Sun* [2000], and *Zhang and Lu* [2002], is based on a perturbation analysis, to transform the stochastic partial differential equations to moment equations. The major problem with the CME method is a substantial requirement of computational resources. For example, to solve the head moments up to first order, the CME method requires the solution of sets of linear algebraic equations with N unknowns for $2N$ times, where N is the number of nodes in the numerical grid [*Zhang and Lu*, 2004]. This requirement limits the application of the method to small-scale simulation problems. *Zhang and Lu* [2004] combined Karhunen-Loeve decomposition with the polynomial expansions and perturbation methods to perform the stochastic analysis of saturated flow. The KLME method decomposes random independent variables (e.g., soil permeability) via the Karhunen-Loeve technique, expands dependent variables into series in different orders, and solves the sets of equations in each order. The solution in each order can be used to construct statistical moments directly. It has been demonstrated that KLME is capable of evaluating higher-order approximations of the dependent variables (pressure and flux) moments and is more efficient and accurate than CME and Monte Carlo approaches [*Zhang and Lu*, 2004; *Lu and Zhang*, 2004b]. *Yang et al.* [2004] extended KLME to analysis of saturated-unsaturated one-phase flow. *Lu and Zhang* [2004a] applied KLME to the conditional simulations of saturated flow. The above three applications of KLME were derived for a two-dimensional domain. *Lu and Zhang* [2005] presented the KLME for a transient saturated flow in a large-scale three-dimensional domain.

[8] *Chen et al.* [2005] introduced the use of KLME for the stochastic analysis of a steady state water-oil two-phase flow system. To simplify the mathematical formulation, the relationship between relative permeability and capillary pressure was defined using an exponential constitutive model instead of the more widely accepted *van Genuchten* [1980] model. The results of the KLME approach compared favorably with those of the Monte Carlo approach for synthetic examples using a small (0.25) and large (0.81) variability of log-transformed intrinsic permeability. The KLME approach was shown to be about 8 times more efficient than the corresponding Monte Carlo simulations.

[9] In this study, we develop a stochastic transient water-oil phase flow model with the van Genuchten constitutive relationship in heterogeneous media using KLME. We first derive a set of differential equations in the zeroth- and first-order by Karhunen-Loeve expansion of independent variables and polynomial expansions of dependent variables and then implement these equations with a finite difference scheme. We then construct the statistical moments of dependent variables, such as water, NAPL, and capillary pressure. Monte Carlo simulations are also conducted to demonstrate the validity of the proposed stochastic model, using the finite element heat and mass (FEHM) transfer code [*Zyvoloski et al.*, 1997]. The stochastic model developed in this study is applicable to the entire domain of a bounded, multidimensional transient water-NAPL phase flow system in the presence of deterministic recharge and sink-source terms.

2. Mechanics of Transient Two-Phase Flow

[10] In this study, the porous medium and fluids are considered incompressible and under isothermal conditions. These assumptions are generally valid for shallow (5–200 m) subsurface transport, where overburden pressure is essentially constant and temperature fluctuations affecting physicochemical properties are negligible [e.g., *Keller and Chen*, 2002]. The conservation equations and Darcy's relationship for the transient water-oil phase flow can be written as [*Abriola and Pinder*, 1985]:

$$\phi \frac{\partial S_l(\mathbf{x},t)}{\partial t} + \nabla \cdot \mathbf{q}_l(\mathbf{x},t) = F_l(\mathbf{x},t), \tag{1}$$

$$\mathbf{q}_l(\mathbf{x},t) = -\lambda_l(\mathbf{x},t)[\nabla P_l(\mathbf{x},t) + \rho_l \mathbf{g}], \tag{2}$$

subject to initial and boundary conditions

$$P_l(\mathbf{x},0) = P_{l0}(\mathbf{x}), \qquad \mathbf{x} \in \Omega, \tag{3}$$

$$P_l(\mathbf{x},t) = P_{lt}(\mathbf{x},t), \qquad \mathbf{x} \in \Gamma_D, \tag{4}$$

$$\mathbf{q}_l(\mathbf{x},t)\cdot\mathbf{n}(\mathbf{x}) = Q_l(\mathbf{x},t), \qquad \mathbf{x} \in \Gamma_N, \tag{5}$$

where l denotes liquids ($l = w, o$); $S_l(\mathbf{x}, t)$ are the water ($l = w$) and oil ($l = o$) saturations; $q_l(\mathbf{x}, t)$ are the water or oil fluxes; $\mathbf{x}$ is the position vector in 2- or 3-D; $F_l(\mathbf{x}, t)$ is a source or sink term; $\lambda_l(\mathbf{x}, t) = k(\mathbf{x})k_{rl}(S_l)/\mu_l$ is liquid mobility; $P_l(\mathbf{x}, t)$ is the fluid pressure; ρ_l is fluid density; $k(\mathbf{x})$ is the intrinsic permeability of porous media; k_{rl} is the water or oil relative permeability; μ_l is the liquid dynamic viscosity; $P_{l0}(\mathbf{x})$ is the initial pressure in the domain Ω; $P_{lt}(\mathbf{x}, t)$ is the prescribed pressure on a Dirichlet boundary segment Γ_D; $Q_l(\mathbf{x}, t)$ is the prescribed fluid flux across Neumann boundary segments Γ_N; $\mathbf{g}$ is the gravity vector; $\mathbf{n}(\mathbf{x})$ is the outward unit vector normal to the boundary Γ_N, and ϕ is the porosity of the media.

[11] Letting $Z_l(\mathbf{x}, t) = \ln \lambda_l(\mathbf{x}, t)$, and combining (1) and (2) gives the governing flow equations as

$$\frac{\partial^2 P_l(\mathbf{x},t)}{\partial x_i^2} + \frac{\partial Z_l(\mathbf{x},t)}{\partial x_i}\left[\frac{\partial P_l(\mathbf{x},t)}{\partial x_i} + \rho_l g \delta_{i1}\right] = \exp[-Z_l(\mathbf{x},t)]\left[\phi\frac{\partial S_l(\mathbf{x},t)}{\partial t} - F_l(\mathbf{x},t)\right], \tag{6}$$

subject to boundary conditions

$$P_l(\mathbf{x},0) = P_{l0}(\mathbf{x}), \qquad \mathbf{x} \in \Omega, \tag{7}$$

$$P_l(\mathbf{x},t) = P_{lt}(\mathbf{x},t), \qquad \mathbf{x} \in \Gamma_D, \tag{8}$$

$$n_i(\mathbf{x})\exp[Z_l(\mathbf{x},t)]\left[\frac{\partial P_l(\mathbf{x},t)}{\partial x_i} + \rho_l g \delta_{i1}\right] = -Q_l(\mathbf{x},t), \qquad \mathbf{x} \in \Gamma_N, \tag{9}$$

where δ_{i1} is the Krönecker delta function, which equals 1 when i is 1 (upward direction) or 0 otherwise.

[12] The capillary pressure-saturation and relative permeability-saturation relations have to be defined. In this study, we use the *van Genuchten* [1980] relationship to describe capillary pressure-saturation functions:

$$\overline{S}_w = [1 + (\alpha P_c)^n]^{-m}, \tag{10}$$

where $\overline{S}_w = (S_w - S_{wr})/(1 - S_{wr})$ is the effective water saturation, $S_w = 1 - S_o$ is water saturation, and S_{wr} is the residual water saturation, α is the pore size distribution, $P_c = P_o - P_w$ is the capillary pressure, n is the van Genuchten fitting parameters and $m = 1 - 1/n$.

[13] The relative permeability-saturation relationship proposed by *Parker and Lenhard* [1990] is the most widely used one in deterministic two-phase flow studies [e.g., *Keller and Chen*, 2003]. *Lu and Zhang* [2002] used the van Genuchten–Mualem constitutive model in their study of applying the CME stochastic approach to transient unsaturated flow, but in the literature of stochastic analysis of multiphase flow, an exponential-type model is usually adopted owing to its mathematic simplicity [*Chang et al.*, 1995; *Abdin and Kaluarachchi*, 1997a, 1997b; *Chen et al.*, 2005]. In this study, we employ Parker and Lenhard's model to the stochastic analysis of the transient water-oil two-phase flow. The functions can be expressed as

$$k_{rw} = \overline{S}_w^{1/2}\left[1 - \left(1 - \overline{S}_w^{1/m}\right)^m\right]^2, \tag{11}$$

$$k_{ro} = \left(1 - \overline{S}_w\right)^{1/2}\left(1 - \overline{S}_w^{1/m}\right)^{2m}. \tag{12}$$

The transient part of the governing equation (6) can be expressed as

$$\phi\frac{\partial S_w}{\partial t} = \phi(1 - S_{wr})\frac{\partial \overline{S}_w}{\partial P_c}\cdot\frac{\partial P_c}{\partial t} = C_{ow}\cdot\frac{\partial P_c}{\partial t}, \tag{13}$$

$$\phi\frac{\partial S_o}{\partial t} = \phi\frac{\partial(1 - S_w)}{\partial t} = -C_{ow}\cdot\frac{\partial P_c}{\partial t}, \tag{14}$$

where

$$C_{ow}(\mathbf{x},t) = \phi(1 - S_{wr})\frac{\partial \overline{S}_w}{\partial P_c} = -\phi(1 - S_{wr})\alpha(n-1)\,\overline{S}_w^{1/m}\left[1 - \overline{S}_w^{1/m}\right]^m. \tag{15}$$

The initial and boundary terms $P_{l0}(\mathbf{x})$ and $P_{lt}(\mathbf{x}, t)$, the source-sink term $D_l(\mathbf{x}, t)$ and ϕ and S_{wr} are assumed to be deterministic. The log-transformed soil permeability $Y(\mathbf{x}) = \ln k(\mathbf{x})$, log pore size distribution parameter $\beta(\mathbf{x}) = \ln \alpha(\mathbf{x})$, and the van Genuchten fitting parameter $\overline{n}(\mathbf{x}) = \ln [n(\mathbf{x}) - 1]$ are treated as random space functions. The parameter $n(\mathbf{x})$ can be guaranteed to be greater than 1 for all values of $\overline{n}(\mathbf{x})$. In turn, the governing equations (1) to (5) become stochastic differential equations, and the corresponding solutions are statistical moments of the dependent variables.

[14] We use a Karhunen-Loeve based moment equation (KLME) approach to solve these stochastic differential equations. In the next section, we describe the Karhunen-Loeve expansion of random soil properties.

3. Karhunen-Loeve Expansion of Random Soil Parameters

[15] The Karhunen-Loeve (KL) expansion [*Karhunen*, 1947; *Loeve*, 1948] of a stochastic process $\alpha(\mathbf{x}, \theta)$, is based on the spectral decomposition of the covariance function of α, $C_\alpha(\mathbf{x}, \mathbf{y})$, with a set of orthogonal polynomials [*Courant and Hilbert*, 1953]. Here, $\mathbf{x}$ and $\mathbf{y}$ indicate spatial locations, while the argument θ denotes the random nature of the corresponding quantity. The covariance function is symmetrical and positive definite. Its eigenfunctions are mutually orthogonal and they form a complete set spanning the function space to which $\alpha(\mathbf{x}, \theta)$ belongs [*Ghanem and*

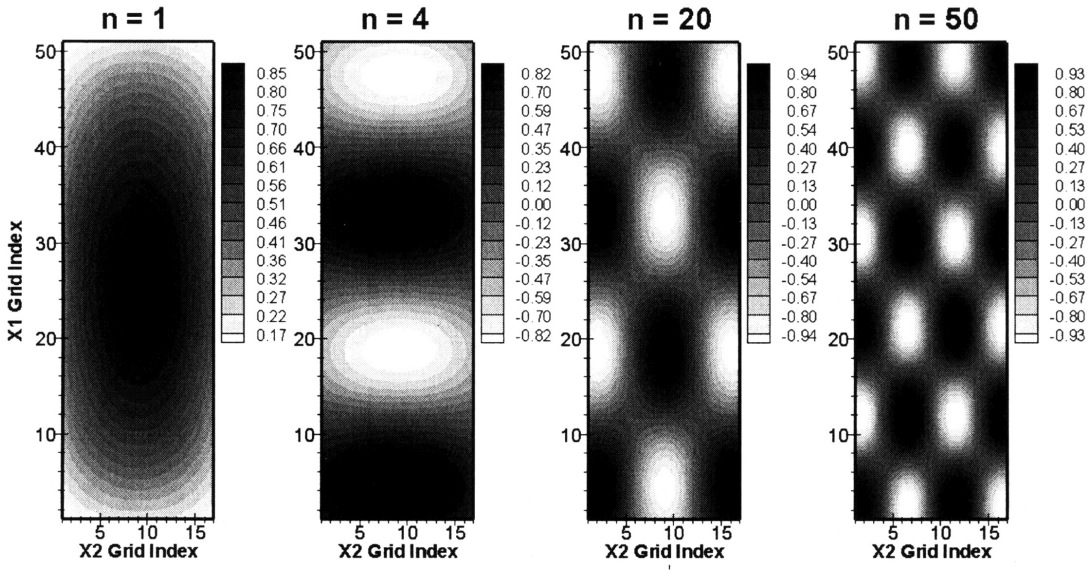

Figure 1. The 1st, 4th, 20th, and 50th eigenfunctions, $\phi_1(\mathbf{x})$, $\phi_4(\mathbf{x})$, $\phi_{20}(\mathbf{x})$, and $\phi_{50}(\mathbf{x})$ from Karhunen-Loeve expansion of the covariance in equation (20), for a two-dimensional random variable.

Dham, 1998]. The perturbation part $\alpha'(\mathbf{x}, \theta)$ represents the fluctuations around the mean $\langle\alpha\rangle$, and can be expanded as follows [*Zhang and Lu*, 2004; *Yang et al.*, 2004; *Chen et al.*, 2005]:

$$\alpha'(\mathbf{x},\theta) = \sum_{n=1}^{\infty} \xi_n(\theta)\sqrt{\lambda_n}\phi_n(\mathbf{x}), \tag{16}$$

where λ_n and $\phi_n(\mathbf{x})$ are the eigenvalues and eigenfunctions of the covariance kernel, respectively. Eigenvalues and eigenfunctions can be solved from the integral equation

$$\int_{\Omega} C_\alpha(\mathbf{x},\mathbf{y})\phi_n(\mathbf{x})d\mathbf{x} = \lambda_n\phi_n(\mathbf{y}), \tag{17}$$

where Ω denotes the spatial domain where $\alpha(\mathbf{x}, \theta)$ is defined.

[16] As defined, $\{\xi_n(\theta)\}$ forms a set of orthogonal random variables, and has properties of $\langle\xi_n(\theta)\rangle = 0$, and $\langle\xi_n(\theta)\xi_m(\theta)\rangle = \delta_{nm}$, where δ_{nm} is the Krönecker delta function. If $\alpha(\mathbf{x}, \theta)$ is assumed Gaussian distributed, $\xi_n(\theta)$ forms a Gaussian vector, and any subset of $\xi_n(\theta)$ is jointly Gaussian, which leads to:

$$\langle\xi_1(\theta)\cdots\xi_{2n+1}(\theta)\rangle = 0, \tag{18}$$

$$\langle\xi_1(\theta)\cdots\xi_{2n}(\theta)\rangle = \sum_{i,j=1}^{2n}\prod\langle\xi_i(\theta)\xi_j(\theta)\rangle. \tag{19}$$

[17] In this study, we use a separable exponential covariance function for a 2-D illustrative example given by

$$C_\alpha(\mathbf{x},\mathbf{y}) = \sigma_\alpha^2 \exp\left(-\frac{|x_1-y_1|}{\eta_1} - \frac{|x_2-y_2|}{\eta_2}\right). \tag{20}$$

where σ_α^2 is the variance of $\alpha(\mathbf{x}, \theta)$, and η_i is the correlation length of $\alpha(\mathbf{x}, \theta)$ in the ith direction. For this kind of covariance function, the analytical solution of eigenvalues and eigenfunctions can be found from (17) [*Zhang and Lu*, 2004]. For the general case, the eigenvalues and eigenfunctions have to be solved numerically via iterative methods or a Galerkin-type method [*Ghanem and Spanos*, 1991]. Figure 1 shows the 1st, 4th, 20th, and 50th eigenfunctions, $\phi_1(\mathbf{x})$, $\phi_4(\mathbf{x})$, $\phi_{20}(\mathbf{x})$, $\phi_{50}(\mathbf{x})$. Figure 2 shows the monotonic decay of the eigenvalues up to λ_{100} with $\sigma_\alpha^2 = 0.25$. The rate of the decay is dependent on the ratios of the correlation length and the domain size in all directions. The smaller the ratio, the more terms are required. Thus, for a nearly white noise process, a large number of terms is necessary to capture the

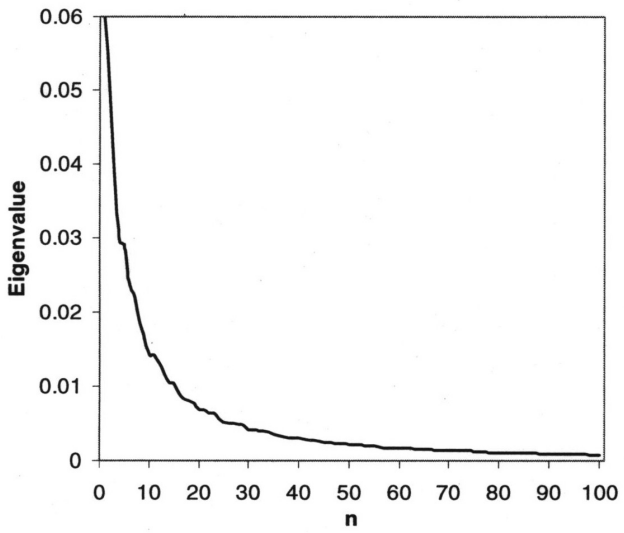

Figure 2. Eigenvalues λ_n from Karhunen-Loeve expansion of covariance of a random variable with variance of 0.25.

uncertainty, while on the other side, only several leading terms can approximate the random variable very well.

[18] In our study, $\alpha(\mathbf{x}, \theta)$ represents the log transformed soil permeability $Y(\mathbf{x})$, pore size distribution $\beta(\mathbf{x})$, or the fitting parameter $\overline{n}(\mathbf{x})$, all of which are assumed to be subject to a Gaussian distribution. As shown in (16), the fluctuations of these three random variables can be expressed in terms of deterministic scales $\phi_n(\mathbf{x})$ multiplied by random amplitudes $\xi_n(\theta)\sqrt{\lambda_n}$.

4. KL-Based Moment Equations

[19] The essence of the KLME approach is the decomposition of the independent random process (e.g., intrinsic permeability) using the KL expansion described in Section 3 and the representation of the dependent stochastic process (fluid pressure) using perturbation methods. With the combination of KL expansion and perturbation methods we derive a series of deterministic differential equations, which are denominated KL-based moment equations (KLME). The solutions of these KLME can be used to construct mean and (co)variances of fluid pressures. In short, the idea of the KLME approach is to decompose stochastic governing equations of flow into a series of deterministic equations, which can be solved using existing numerical techniques. The solutions are then assembled to obtain explicit and intelligible moments to investigate the uncertainty of the dependent variables.

[20] In this section, we derive a set of KLME up to first order for transient water-oil two-phase flow. On the basis of $\lambda_l(\mathbf{x}, t) = k(\mathbf{x})k_{rl}(S_l)/\mu_l$ and equations (11), (12), the log transformed water and oil phase mobility $Z_l = \ln \lambda_l$ can be derived as

$$Z_w = \ln \lambda_w = Y - \ln \mu_w + \frac{1}{2} \ln \overline{S}_w + 2 \ln\left[1 - \left(1 - \overline{S}_w^{1/m}\right)^m\right], \tag{21}$$

$$Z_o = \ln \lambda_o = Y - \ln \mu_o + \frac{1}{2} \ln\left(1 - \overline{S}_w\right) + 2m \ln\left(1 - \overline{S}_w^{1/m}\right). \tag{22}$$

Substituting (13) and (14) into (6) yields

$$\frac{\partial^2 P_w(\mathbf{x},t)}{\partial x_i^2} + \frac{\partial Z_w(\mathbf{x},t)}{\partial x_i}\left[\frac{\partial P_w(\mathbf{x},t)}{\partial x_i} + \rho_w g \delta_{i1}\right] = \frac{C_{ow}(\mathbf{x},t)}{\exp[Z_w(\mathbf{x},t)]} \cdot \frac{\partial P_c(\mathbf{x},t)}{\partial t} - \frac{F_w(\mathbf{x},t)}{\exp[Z_w(\mathbf{x},t)]}, \tag{23}$$

$$\frac{\partial^2 P_o(\mathbf{x},t)}{\partial x_i^2} + \frac{\partial Z_o(\mathbf{x},t)}{\partial x_i}\left[\frac{\partial P_o(\mathbf{x},t)}{\partial x_i} + \rho_o g \delta_{i1}\right] = \frac{-C_{ow}(\mathbf{x},t)}{\exp[Z_o(\mathbf{x},t)]} \cdot \frac{\partial P_c(\mathbf{x},t)}{\partial t} - \frac{F_o(\mathbf{x},t)}{\exp[Z_o(\mathbf{x},t)]}. \tag{24}$$

The boundary conditions are the same as those shown in (7), (8) and (9). One may expand them into infinite series: $P_l(\mathbf{x}, t) = P_l^{(0)} + P_l^{(1)} + \cdots$, $P_c(\mathbf{x}, t) = P_c^{(0)} + P_c^{(1)} + \cdots$, $Z_l(\mathbf{x}, t) = Z_l^{(0)} + Z_l^{(1)} + \cdots$, and $C_{ow}(\mathbf{x}, t) = C_{ow}^{(0)} + C_{ow}^{(1)} + \cdots$. In these series, the order of each term is with respect to σ_s, which is some combination of the variability of the input variables. Substituting these decompositions into (23) and (24), and collecting terms at the same order generates the differential equations for zeroth order:

$$\frac{\partial^2 P_w^{(0)}(\mathbf{x},t)}{\partial x_i^2} + \frac{\partial Z_w^{(0)}(\mathbf{x},t)}{\partial x_i}\left[\frac{\partial P_w^{(0)}(\mathbf{x},t)}{\partial x_i} + \rho_w g \delta_{i1}\right] = \frac{C_{ow}^{(0)}(\mathbf{x},t)}{\exp\left[Z_w^{(0)}(\mathbf{x},t)\right]} \cdot \frac{\partial P_c^{(0)}(\mathbf{x},t)}{\partial t} - \frac{F_w(\mathbf{x},t)}{\exp\left[Z_w^{(0)}(\mathbf{x},t)\right]}, \tag{25}$$

$$\frac{\partial^2 P_o^{(0)}(\mathbf{x},t)}{\partial x_i^2} + \frac{\partial Z_o^{(0)}(\mathbf{x},t)}{\partial x_i}\left[\frac{\partial P_o^{(0)}(\mathbf{x},t)}{\partial x_i} + \rho_o g \delta_{i1}\right] = \frac{-C_{ow}^{(0)}(\mathbf{x},t)}{\exp\left[Z_o^{(0)}(\mathbf{x},t)\right]} \cdot \frac{\partial P_c^{(0)}(\mathbf{x},t)}{\partial t} - \frac{F_o(\mathbf{x},t)}{\exp\left[Z_o^{(0)}(\mathbf{x},t)\right]}, \tag{26}$$

$$P_l^{(0)}(\mathbf{x}, 0) = P_{l0}(\mathbf{x}), \qquad \mathbf{x} \in \Omega, \tag{27}$$

$$P_l^{(0)}(\mathbf{x}, t) = P_{lt}(\mathbf{x}, t), \qquad \mathbf{x} \in \Gamma_D, \tag{28}$$

$$n_i(\mathbf{x})\left[\frac{\partial P_l^{(0)}(\mathbf{x},t)}{\partial x_i} + \rho_l g \delta_{i1}\right] = \frac{-Q_l(\mathbf{x},t),}{\exp\left[Z_l^{(0)}(\mathbf{x},t)\right]}, \qquad \mathbf{x} \in \Gamma_N \tag{29}$$

and for first order:

$$\frac{\partial^2 P_w^{(1)}(\mathbf{x},t)}{\partial x_i^2} + J_{wi}(\mathbf{x},t)\frac{\partial Z_w^{(1)}(\mathbf{x},t)}{\partial x_i} + \frac{\partial Z_w^{(0)}(\mathbf{x},t)}{\partial x_i}\frac{\partial P_w^{(1)}(\mathbf{x},t)}{\partial x_i} = \cdot \frac{C_{ow}^{(0)}(\mathbf{x},t)}{\exp\left[Z_w^{(0)}(\mathbf{x},t)\right]}\left[\frac{\partial P_c^{(1)}(\mathbf{x},t)}{\partial t} - Z_w^{(1)}(\mathbf{x},t)\frac{\partial P_c^{(0)}(\mathbf{x},t)}{\partial t}\right] + \frac{C_{ow}^{(1)}(\mathbf{x},t)}{\exp\left[Z_w^{(0)}(\mathbf{x},t)\right]}\frac{\partial P_c^{(0)}(\mathbf{x},t)}{\partial t} - \frac{F_w(\mathbf{x},t)}{\exp\left[Z_w^{(0)}(\mathbf{x},t)\right]}Z_w^{(1)}(\mathbf{x},t), \tag{30}$$

$$\frac{\partial^2 P_o^{(1)}(\mathbf{x},t)}{\partial x_i^2} + J_{oi}(\mathbf{x},t)\frac{\partial Z_o^{(1)}(\mathbf{x},t)}{\partial x_i} + \frac{\partial Z_o^{(0)}(\mathbf{x},t)}{\partial x_i}\frac{\partial P_o^{(1)}(\mathbf{x},t)}{\partial x_i} = \frac{-C_{ow}^{(0)}(\mathbf{x},t)}{\exp\left[Z_o^{(0)}(\mathbf{x},t)\right]}\left[\frac{\partial P_c^{(1)}(\mathbf{x},t)}{\partial t} - Z_o^{(1)}(\mathbf{x},t)\frac{\partial P_c^{(0)}(\mathbf{x},t)}{\partial t}\right] - \frac{C_{ow}^{(1)}(\mathbf{x},t)}{\exp\left[Z_o^{(0)}(\mathbf{x},t)\right]}\frac{\partial P_c^{(0)}(\mathbf{x},t)}{\partial t} - \frac{F_o(\mathbf{x},t)}{\exp\left[Z_o^{(0)}(\mathbf{x},t)\right]}Z_o^{(1)}(\mathbf{x},t), \tag{31}$$

$$P_l^{(1)}(\mathbf{x}, 0) = 0, \qquad \mathbf{x} \in \Omega, \tag{32}$$

$$P_l^{(1)}(\mathbf{x}, t) = 0, \qquad \mathbf{x} \in \Gamma_D, \tag{33}$$

$$n_i(\mathbf{x})\left[\frac{\partial P_l^{(1)}(\mathbf{x},t)}{\partial x_i} + J_{li}(\mathbf{x},t)Z_l^{(1)}(\mathbf{x},t)\right] = 0, \qquad \mathbf{x} \in \Gamma_N, \tag{34}$$

where $J_{li}(\mathbf{x}, t) = \partial P_l^{(0)}(\mathbf{x}, t)/\partial x_i + \rho_l g \delta_{i1}$ ($l = w, o$) is the spatial mean gradient of total water and oil pressure. On the basis of (21), (22) and (15), we can obtain

$$Z_w^{(0)}(\mathbf{x}, t) = Y - \ln \mu_w + \frac{1}{2} \ln \overline{S}_w^{(0)} + 2 \ln \left[1 - \left(1 - \overline{S}_w^{(0)1/\langle m \rangle} \right)^{\langle m \rangle} \right], \tag{35}$$

$$Z_o^{(0)}(\mathbf{x}, t) = Y - \ln \mu_o + \frac{1}{2} \ln \left(1 - \overline{S}_w^{(0)} \right) + 2\langle m \rangle \ln \left(1 - \overline{S}_w^{(0)1/\langle m \rangle} \right), \tag{36}$$

$$C_{ow}(\mathbf{x}, t) = -\phi (1 - S_{wr}) e^{\langle \beta \rangle} e^{\langle \overline{n} \rangle} \overline{S}_w^{(0)1/\langle m \rangle} \left[1 - \overline{S}_w^{(0)1/\langle m \rangle} \right]^{\langle m \rangle}, \tag{37}$$

and

$$Z_w^{(1)}(\mathbf{x}, t) = Y' + u_{w,100} P_c^{(1)} + u_{w,010} \beta' + u_{w,001} \overline{n}' \tag{38}$$

$$Z_o^{(1)}(\mathbf{x}, t) = Y' + u_{o,100} P_c^{(1)} + u_{o,010} \beta' + u_{o,001} \overline{n}' \tag{39}$$

$$C_{ow}^{(1)}(\mathbf{x}, t) = v_{100} P_c^{(1)} + v_{010} \beta' + v_{001} \overline{n}' \tag{40}$$

where

$$u_{w,ijk}(\mathbf{x}, t) = \frac{\partial^{i+j+k} Z_w(\mathbf{x}, t)}{\partial P_c^i \partial \beta^j \partial \overline{n}^k}, \tag{41}$$

$$u_{o,ijk}(\mathbf{x}, t) = \frac{\partial^{i+j+k} Z_o(\mathbf{x}, t)}{\partial P_c^i \partial \beta^j \partial \overline{n}^k}, \tag{42}$$

$$v_{ijk}(\mathbf{x}, t) = \frac{\partial^{i+j+k} C_{ow}(\mathbf{x}, t)}{\partial P_c^i \partial \beta^j \partial \overline{n}^k}. \tag{43}$$

(41), (42) and (43) are evaluated at $P_c^{(0)}(\mathbf{x}, t)$, $\langle \beta(\mathbf{x}) \rangle$, and $\langle \overline{n}(\mathbf{x}) \rangle$, and their explicit expressions are given in the auxiliary material.[1] On the basis of (16), the KL expansion of the fluctuation part of log transformed soil permeability can be expressed as:

$$Y'(\mathbf{x}, \theta) = \sum_{n=1}^{\infty} \xi_n(\theta) \sqrt{\lambda_n} f_n(\mathbf{x}) = \sum_{n=1}^{\infty} \xi_n(\theta) \overline{f}_n(\mathbf{x}) \tag{44}$$

In the above equation, $\sqrt{\lambda_n}$ and $f_n(\mathbf{x})$ are combined into $\overline{f}_n(\mathbf{x})$, since $\sqrt{\lambda_n}$ and $f_n(\mathbf{x})$ are always coupled. $\overline{f}_n(\mathbf{x})$ will be written as $f_n(\mathbf{x})$ in the following formulation for simplicity. Similarly, the KL expansion of the log pore size distribution parameter $\beta(\mathbf{x})$, and van Genuchten fitting parameter $\overline{n}(\mathbf{x})$ are:

$$\beta'(\mathbf{x}, \theta) = \sum_{n=1}^{\infty} \xi_n(\theta) \phi_n(\mathbf{x}) \tag{45}$$

$$\overline{n}'(\mathbf{x}, \theta) = \sum_{n=1}^{\infty} \xi_n(\theta) \psi_n(\mathbf{x}) \tag{46}$$

where $\phi_n(\mathbf{x})$ and $\psi_n(\mathbf{x})$ are respectively the product of the square root of an eigenvalue and its corresponding eigenfunction of covariance $C_\beta(\mathbf{x}, \mathbf{y})$ and $C_{\overline{n}}(\mathbf{x}, \mathbf{y})$.

[21] We assume that $P_l^{(1)}(\mathbf{x}, t)$, $Z_l^{(1)}(\mathbf{x}, t)$, and $C_{ow}^{(1)}(\mathbf{x}, t)$ can be expressed in terms of a set of orthogonal Gaussian random variables $\{\xi_n\}$ and deterministic coefficients $P_{l,n}^{(1)}(\mathbf{x}, t)$, $Z_{l,n}^{(1)}(\mathbf{x}, t)$, and $C_{ow,n}^{(1)}(\mathbf{x}, t)$:

$$P_l^{(1)}(\mathbf{x}, t) = \sum_{n=1}^{\infty} \xi_n P_{l,n}^{(1)}(\mathbf{x}, t) \tag{47}$$

$$Z_l^{(1)}(\mathbf{x}, t) = \sum_{n=1}^{\infty} \xi_n Z_{l,n}^{(1)}(\mathbf{x}, t) \tag{48}$$

$$C_{ow}^{(1)}(\mathbf{x}, t) = \sum_{n=1}^{\infty} \xi_n C_{ow,n}^{(1)}(\mathbf{x}, t) \tag{49}$$

Substituting (47), (48), and (49) into (30) to (34) yields the infinite series of $\{\xi_n\}$ on both sides. Multiplying ξ_n on both sides of the derived equations and taking the ensemble means yields:

$$\begin{aligned} &\frac{\partial^2 P_{w,n}^{(1)}(\mathbf{x}, t)}{\partial x_i^2} + J_{wi}(\mathbf{x}, t) \frac{\partial Z_{w,n}^{(1)}(\mathbf{x}, t)}{\partial x_i} + \frac{\partial Z_w^{(0)}(\mathbf{x}, t)}{\partial x_i} \frac{\partial P_{w,n}^{(1)}(\mathbf{x}, t)}{\partial x_i} = \\ &\quad \frac{C_{ow}^{(0)}(\mathbf{x}, t)}{\exp\left[Z_w^{(0)}(\mathbf{x}, t) \right]} \left[\frac{\partial P_{c,n}^{(1)}(\mathbf{x}, t)}{\partial t} - Z_{w,n}^{(1)}(\mathbf{x}, t) \frac{\partial P_c^{(0)}(\mathbf{x}, t)}{\partial t} \right] \\ &\quad + \frac{C_{ow,n}^{(1)}(\mathbf{x}, t)}{\exp\left[Z_w^{(0)}(\mathbf{x}, t) \right]} \frac{\partial P_c^{(0)}(\mathbf{x}, t)}{\partial t} - \frac{F_w(\mathbf{x}, t)}{\exp\left[Z_w^{(0)}(\mathbf{x}, t) \right]} Z_{w,n}^{(1)}(\mathbf{x}, t), \end{aligned} \tag{50}$$

$$\begin{aligned} &\frac{\partial^2 P_{o,n}^{(1)}(\mathbf{x}, t)}{\partial x_i^2} + J_{oi}(\mathbf{x}, t) \frac{\partial Z_{o,n}^{(1)}(\mathbf{x}, t)}{\partial x_i} + \frac{\partial Z_o^{(0)}(\mathbf{x}, t)}{\partial x_i} \frac{\partial P_{o,n}^{(1)}(\mathbf{x}, t)}{\partial x_i} = \\ &\quad \frac{-C_{ow}^{(0)}(\mathbf{x}, t)}{\exp\left[Z_o^{(0)}(\mathbf{x}, t) \right]} \left[\frac{\partial P_{c,n}^{(1)}(\mathbf{x}, t)}{\partial t} - Z_{o,n}^{(1)}(\mathbf{x}, t) \frac{\partial P_c^{(0)}(\mathbf{x}, t)}{\partial t} \right] \\ &\quad - \frac{C_{ow,n}^{(1)}(\mathbf{x}, t)}{\exp\left[Z_o^{(0)}(\mathbf{x}, t) \right]} \frac{\partial P_c^{(0)}(\mathbf{x}, t)}{\partial t} - \frac{F_o(\mathbf{x}, t)}{\exp\left[Z_o^{(0)}(\mathbf{x}, t) \right]} Z_{o,n}^{(1)}(\mathbf{x}, t), \end{aligned} \tag{51}$$

$$P_{l,n}^{(1)}(\mathbf{x}, 0) = 0, \qquad l = \mathrm{w}, \mathrm{o}, \quad \mathbf{x} \in \Omega, \tag{52}$$

$$P_{l,n}^{(1)}(\mathbf{x}, t) = 0, \qquad l = \mathrm{w}, \mathrm{o}, \quad \mathbf{x} \in \Gamma_D, \tag{53}$$

$$n_i(\mathbf{x}) \left[\frac{\partial P_{l,n}^{(1)}(\mathbf{x}, t)}{\partial x_i} + J_{li}(\mathbf{x}, t) Z_{l,n}^{(1)}(\mathbf{x}, t) \right] = 0, \quad l = \mathrm{w}, \mathrm{o}, \quad \mathbf{x} \in \Gamma_N, \tag{54}$$

[1] Auxiliary material is available at ftp://ftp.agu.org/apend/wr/2005wr004257.

where, on the basis of (38) to (40) and (44) to (46),

$$Z^{(1)}_{w,n}(\mathbf{x},t) = f_n + u_{w,100}P^{(1)}_{c,n} + u_{w,010}\phi_n + u_{w,001}\psi_n, \quad (55)$$

$$Z^{(1)}_{o,n}(\mathbf{x},t) = f_n + u_{o,100}P^{(1)}_{c,n} + u_{o,010}\phi_n + u_{o,001}\psi_n, \quad (56)$$

$$C^{(1)}_{ow,n}(\mathbf{x},t) = v_{100}P^{(1)}_{c,n} + v_{010}\phi_n + v_{001}\psi_n. \quad (57)$$

In this study, we approximate liquid pressure up to first order in σ_s:

$$P_l(\mathbf{x},t) \approx P^{(0)}_l(\mathbf{x},t) + P^{(1)}_l(\mathbf{x},t). \quad (58)$$

The zeroth-order mean liquid pressure is shown as

$$\langle P_l(\mathbf{x},t)\rangle \approx \left\langle P^{(0)}_l(\mathbf{x},t)\right\rangle + \left\langle P^{(1)}_l(\mathbf{x},t)\right\rangle = P^{(0)}_l(\mathbf{x},t). \quad (59)$$

Hence the fluctuation of liquid pressure is

$$P'_l(\mathbf{x},t) \approx P_l(\mathbf{x},t) - \langle P_l(\mathbf{x},t)\rangle = P^{(1)}_l(\mathbf{x},t). \quad (60)$$

The covariance of liquid pressure up to first order can be derived as

$$C_{P_l}(\mathbf{x},\mathbf{y},t) = \sum_{n=1}^{\infty} P^{(1)}_{l,n}(\mathbf{x},t)P^{(1)}_{l,n}(\mathbf{y},t). \quad (61)$$

It is apparent that we can construct the statistical moments of water, oil and capillary pressure from the zeroth-order solution of (25) to (29) and the first-order solution of (50) to (54). We use a finite difference scheme to discretize these nonlinear and/or coupled differential equations and incorporate the related code to the stochastic two-phase numerical model "STO-2PHASE", which was developed by *Chen et al.* [2005].

5. Illustrative Examples

[22] In this section, we demonstrate the KLME model developed here to the study of transient water-NAPL flow in a hypothetical heterogeneous soil using two examples. We assume the log intrinsic permeability $Y(\mathbf{x})$, log pore size distribution parameter $\beta(\mathbf{x})$, and log van Genuchten fitting parameter $\overline{n}(\mathbf{x})$ to be random fields with an exponential covariance function following equation (20).

[23] We consider the model domain adopted by *Chen et al.* [2005]. It is a rectangle of 3 m by 0.96 m in a vertical cross section, discretized into 50 × 16 square elements of 0.06 m × 0.06 m. The boundary condition are specified as follows: (1) no flow on the sides (X2 = 0, X2 = 0.96 m); (2) constant deterministic water and oil infiltration rates Q_w, Q_o can occur at the top boundary (X1 = 3.0 m); and (3) the water and oil phase pressure P_w, P_o are specified at the bottom of the domain (X1 = 0.0 m) (Figure 3). We refer to the study by *Chang et al.* [1995] to choose the values of the input parameters (Table 1). NAPL source is leaked into the domain at node X1 = 2.4 m, X2 = 0.48 m (black solid circle in Figure 3) and a constant precipitation rate is fixed at the top boundary. The soil porosity is 0.5 and the residual water saturation is 0.04. The initial water saturation is 0.993 across the domain, which means a unique value of 200 Pa of capillary pressure everywhere. The coefficient of variation (CV) of the intrinsic permeability, pore size distribution parameter, and fitting parameter are 53.29%, 10.03%, and 7.86%, respectively. The initial values and boundary conditions represent a continuous NAPL leak into the nearly clean soil (initial NAPL saturation < 0.01) with constant precipitation on the soil surface. In case 1, we consider 100 kg/day of NAPL leakage and a water infiltration rate of 10^{-9} m/s. To test the model under different conditions, in case 2 we consider a smaller NAPL leakage (8 kg/day) and larger water infiltration rate (1.9×10^{-8} m/s). Case 1 is representative of a pipeline leak in a dry climate (e.g., California), while case 2 is typical of an underground

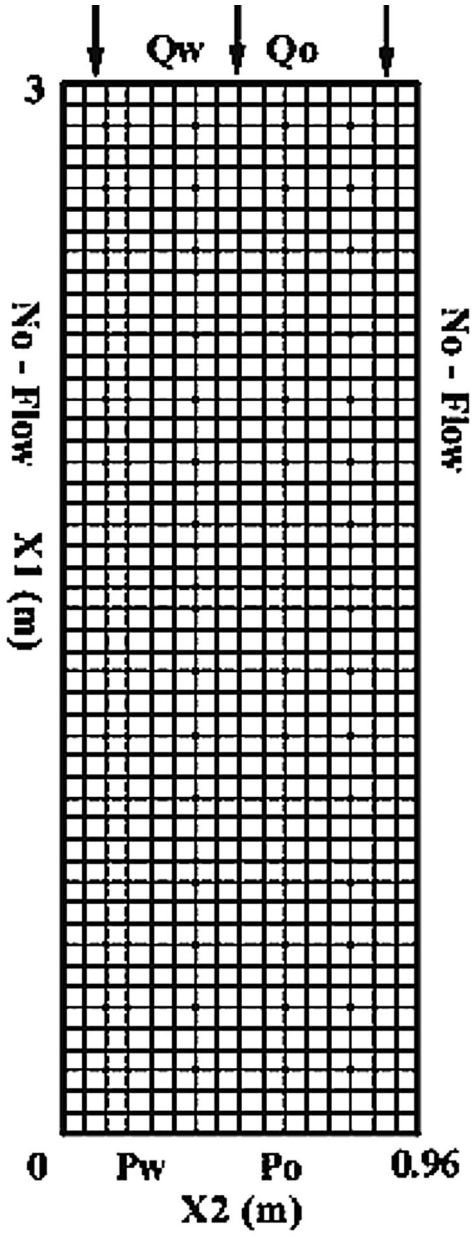

Figure 3. Model domain and boundary configuration.

Table 1. Soil and Fluid Properties and Boundary Conditions

Parameter Name	Symbol	Units	Case 1	Case 2
Water density	ρ_w	kg/m^3	997.81	997.81
Oil density	ρ_o	kg/m^3	800	800
Water viscosity	μ_w	Pa s	1.0×10^{-3}	1.0×10^{-3}
Oil viscosity	μ_o	Pa s	6.5×10^{-4}	6.5×10^{-4}
Mean intrinsic permeability	$\langle k \rangle$	m^2	1.88×10^{-12}	1.88×10^{-12}
Mean pore size distribution	$\langle \alpha \rangle$	1/Pa	2.03×10^{-4}	2.03×10^{-4}
Mean fitting parameter n	$\langle n \rangle$		1.35	1.35
Variance of permeability	σ_k^2		1.29×10^{-24}	1.29×10^{-24}
Variance of pore size distribution	σ_α^2		4.20×10^{-10}	4.20×10^{-10}
Variance of fitting parameter n	σ_n^2		1.13×10^{-2}	1.13×10^{-2}
Coefficient of variation (k)	$CV(k)$		53.29 %	53.29 %
Coefficient of variation (α)	$CV(\alpha)$		10.03 %	10.03 %
Coefficient of variation (n)	$CV(n)$		7.86 %	7.86 %
Correlation length	η_k, η_α, η_n	m	0.3	0.3
Lower boundary water pressure	P_w	Pa	5.00×10^4	5.00×10^4
Lower boundary oil pressure	P_o	Pa	5.02×10^4	5.02×10^4
Upper boundary water flux	Q_w	m/s	1.0×10^{-10}	1.93×10^{-8}
Oil leakage rate	F_o	kg/d	100	8

storage tank leak under humid climatic conditions (e.g., East Coast of United States).

[24] To test the validity of the KLME approach and the numerical implementation, we conducted 2000 Monte Carlo (MC) simulations for case 1. The approximate number of MC runs required was determined by plotting the mean and/or variance of the dependent variables at some selected locations and examining their convergence. The statistical

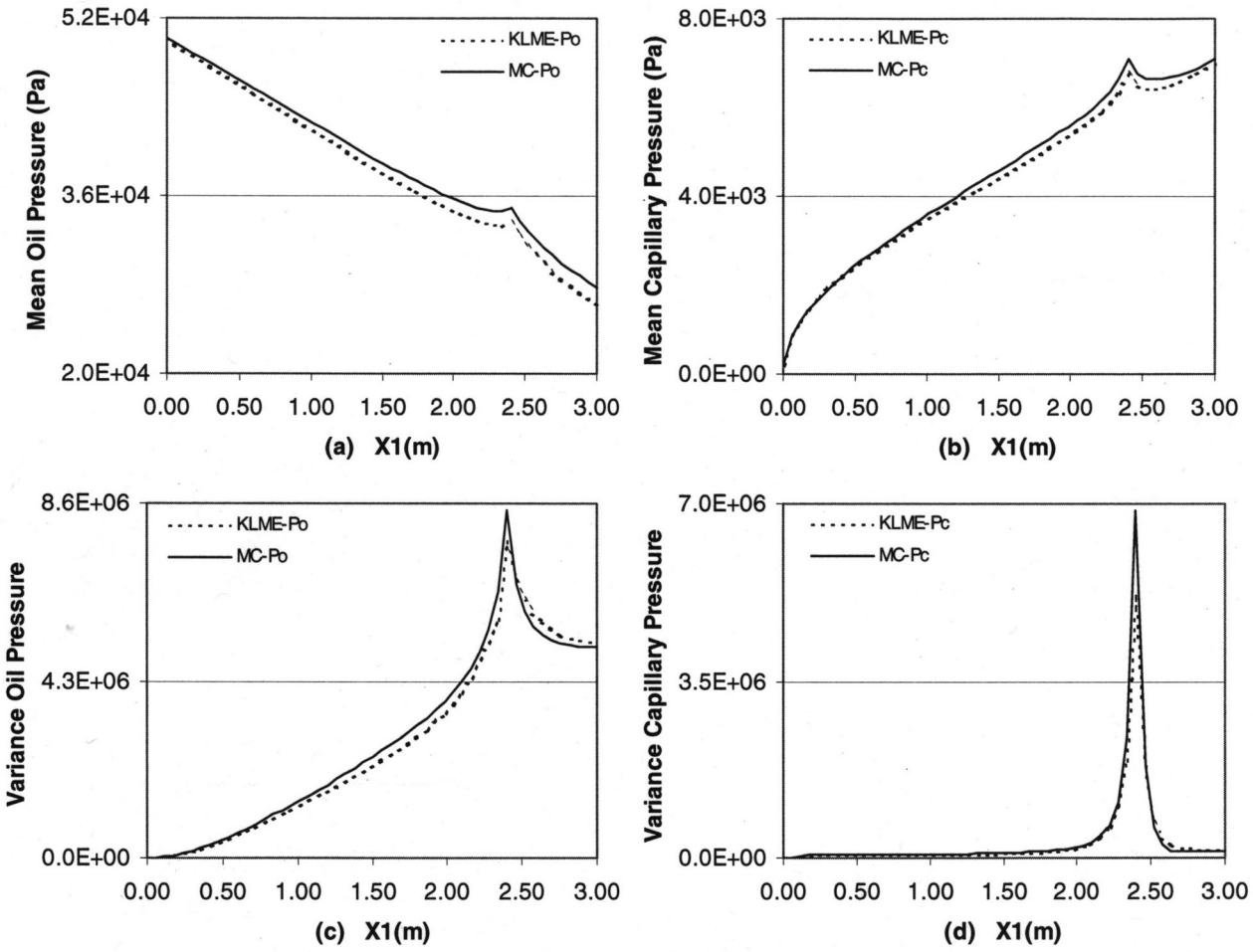

Figure 4. Comparison between Monte Carlo simulations (solid line) and KLME simulations (dashed line) at 1.0 day for mean (a) oil pressure and (b) capillary pressure, and variances of (c) oil pressure, and (d) capillary pressure.

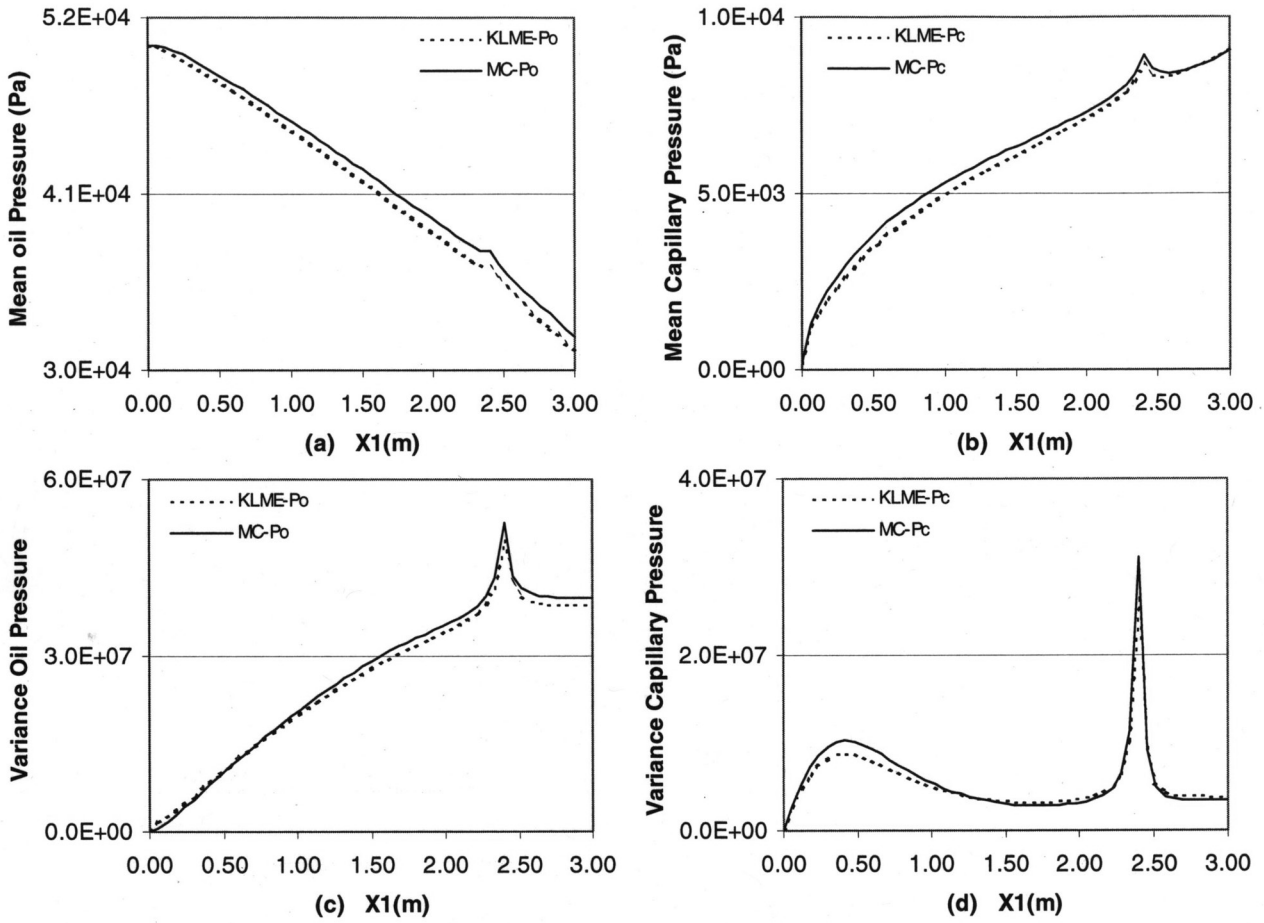

Figure 5. Comparison between Monte Carlo simulations (solid line) and KLME simulations (dashed line) at 10 day for mean (a) oil pressure and (b) capillary pressure and variances of (c) oil pressure and (d) capillary pressure.

moments computed from the 2000 MC realizations are considered ''true'' solutions as a reference for comparing to the KLME results. We first generated 2000 unconditional realizations with zero-mean, unit variance, and given the covariance function as shown in (20), using the sequential Gaussian simulation approach (sgsim) available in GSLIB [*Deutsch and Journel*, 1992]. For each simulation, a two-dimensional log intrinsic permeability $Y(\mathbf{x})$, log pore size distribution parameter $\beta(\mathbf{x})$, and log van Genuchten fitting parameter $\overline{n}(\mathbf{x}) = \ln [n(\mathbf{x}) - 1]$ fields are read from (0, 1) normal distribution and scaled to the specific mean and variance for two different cases. The transient water-oil flow system Equations (1) to (5) are solved using FEHM for each set of $Y(\mathbf{x})$, $\beta(\mathbf{x})$, and $\overline{n}(\mathbf{x})$realizations.

5.1. Case 1

[25] Figure 4, 5, and 6 illustrate the comparison of central vertical profiles of mean oil and capillary pressure between the Monte Carlo (MC) simulations and the KLME stochastic approach at 1.0, 10 and 100 days, respectively. Note that the scale on the y axis changes with time, to reflect the oil and capillary pressures. It is seen that the mean pressures derived from the stochastic model closely match the MC simulation, and the discrepancies decrease with time (Table 2). For example, the average differences in mean capillary pressure between KLME and MC are 5.66%, 4.80% and 2.48% at time of 1.0, 10, and 100 day respectively. These discrepancies result from the numerical errors in solving the governing equations and neglecting higher-order terms in the KLME approach, and the statistical errors in representing soil heterogeneities by a limited number of Monte Carlo realizations. With increasing simulation time, numerical errors from the transient part of the governing equations decrease, resulting in a closer match between MC and KLME. The mean oil pressure is fixed as 50200 Pa at X1 = 0 m for all X2, and decreases with the elevation (X1), with a slight increase at the oil leak; the variance of the oil pressure is zero at the lower boundary and increases with X1, spiking at the injection point. The sharpness of the peak decreases with time despite the continuous oil leak. This is probably caused by constant water infiltration at the top boundary, which dampens the effect of oil leakage 0.6 m below. The mean oil pressure profile becomes curvilinear in the region below the location of the oil leak as time increases (Figures 5 and 6), as the overall oil pressure increases in the upper region of the domain but remains constant at the bottom. The mean capillary pressure is assigned an initial value of 200 Pa across the whole domain, and the value is fixed at the bottom boundary throughout

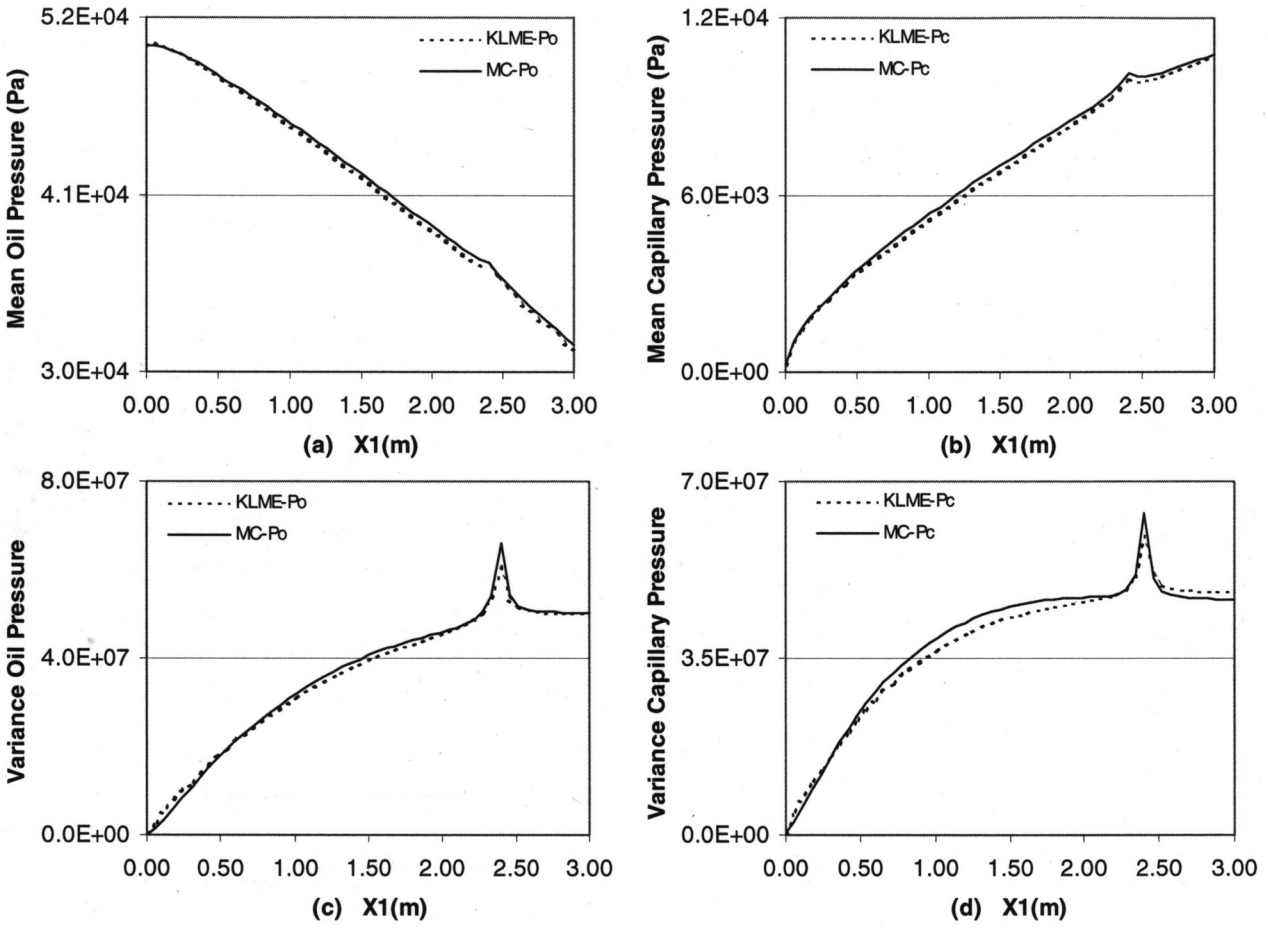

Figure 6. Comparison between Monte Carlo simulations (solid line) and KLME simulations (dashed line) at 100 day for mean (a) oil pressure and (b) capillary pressure and variances of (c) oil pressure and (d) capillary pressure.

the modeling time. At time of 1.0 day (Figure 4), the mean capillary pressure in the lower part of the domain increases significantly from the initial value, reaching a peak at the location of the oil leak. At early times (e.g., t = 1.0 day), there is almost no variance in capillary pressure except at the injection point. The sharpness of the peaks in mean and variance for the capillary pressure decreases with time (Figures 4–6).

[26] As indicated in Table 2, the average differences in variance between MC and KLME are higher than the differences in mean pressures. The average difference in variance decreases with time. For example, the average differences in capillary pressure variance are 15.8%, 10.5%, and 7.69% at the three time points. The differences in variance for capillary pressure are larger than that for the oil pressure, with the most of the differences in the two models near the injection point. This may be explained by the approximations made in the KLME stochastic approach. Because of the mathematic complexity of the higher-order approximation, we derive the stochastic transient two-phase flow only to first order, which may be enough to capture the overall behavior and large-scale fluctuations of the random fields. The resulting stochastic model may, however, have difficulty capturing the drastic changes near the injection point without the higher-order correction. It is believed that the differences in mean and variance of the pressures would be reduced considerably with the second-order term, as was used by *Chen et al.* [2005] for the simpler steady state case with exponential constitutive model. However, the KLME model results compare favorably with the MC model results if the objective is to understand the movement of the NAPL leak into a heterogeneous aquifer.

[27] Figures 7 and 8 present the 2-D contour maps of the mean and variance of capillary pressure at 0.1, 1.0, and 100 days. The mean capillary pressure field increases with time; the initial depression due to the initiation of the oil leak at t = 0.1 day spreads out at 1.0 day and is further dampened

Table 2. Average Relative Difference Between Results From Monte Carlo Simulations and the KLME Stochastic Approach for Case 1

Time, days	Mean(Pw)	Mean(Po)	Mean(Pc)	var(Pw)	var(Po)	var(Pc)
0.1	1.92%	2.28%	7.88%	7.94%	8.90%	18.7%
1.0	1.84%	1.64%	5.66%	7.26%	8.84%	15.8%
10	1.40%	1.56%	4.80%	7.00%	7.78%	10.5%
100	0.355%	0.499%	2.48%	6.86%	7.23%	7.69%

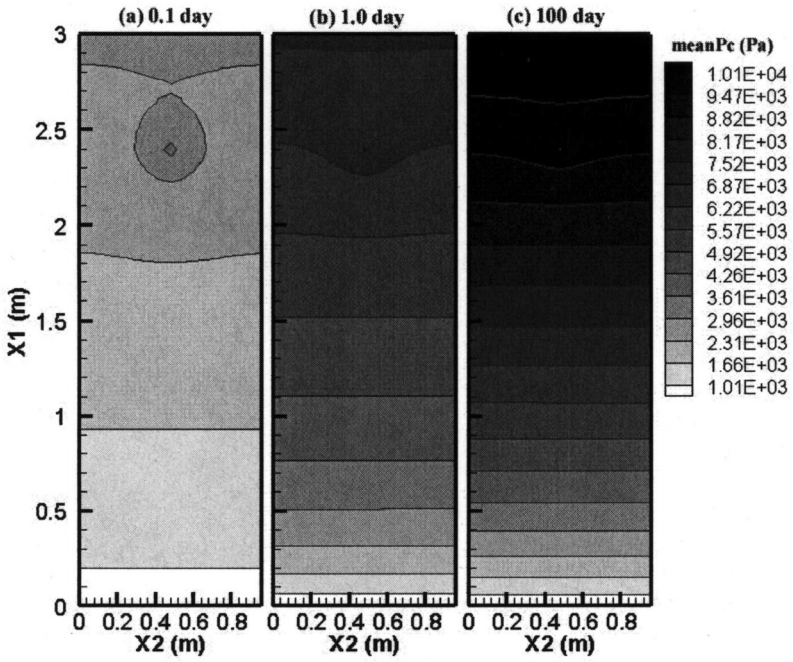

Figure 7. Contour maps of mean capillary pressure fields for case 1 at (a) 0.1 days, (b) 1.0 day, and (c) 100 days.

at 100 day, even though oil continues to enter the domain (Figure 7). The variance does reflect significant repercussions both temporally and spatially (Figure 8). The initial effect of the oil leak is very localized (Figure 8a) and stays fairly constant even at 1.0 day (Figure 8b) but spreads to influence the variance of capillary pressure throughout the entire domain after 100 day, although with the peak centered at the injection point (Figure 8c). Although the soil properties are randomly distributed, the mean and variance are symmetrically distributed throughout the domain.

5.2. Case 2

[28] In this case, the oil leak rate was decreased approximately one order of magnitude and the water infiltration

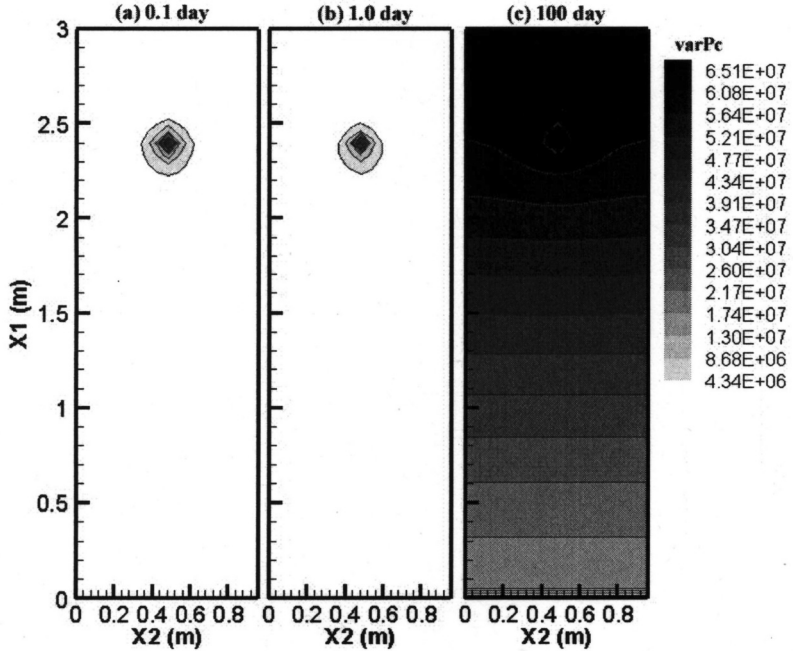

Figure 8. Contour maps of variances of capillary pressure fields for case 1 at (a) 0.1 days, (b) 1.0 day, and (c) 100 days.

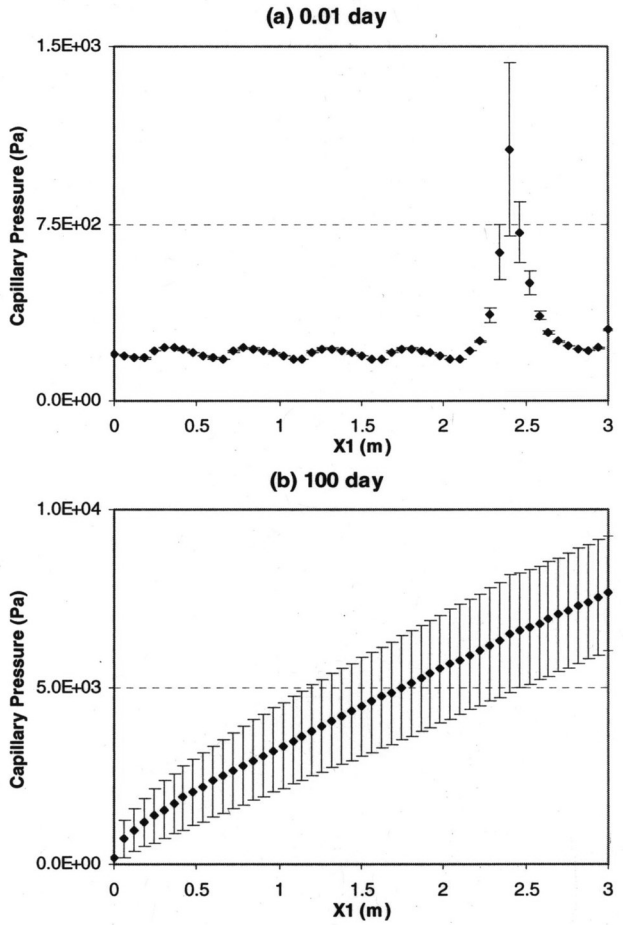

Figure 9. Central vertical profiles of mean and standard deviation of capillary pressures in case 2 at time of (a) 0.01 days and (b) 100 days. A standard deviation for each node is plotted with the error bars.

rate was increased. Figure 9 presents the mean capillary pressure error bars of one standard deviation, based on the calculated variance, at each node along the central vertical line of the domain at 0.01 and 100 days. Compared to case 1, the capillary pressure peak is smaller at 0.01 day at the oil leakage location, but is still very sharp. The variance in capillary pressure also is large around the oil injection node. The peak almost completely disappears after 100 days.

[29] The mean and variance of the water saturation field at 0.01, 0.1 and 100 days are presented in Figure 10. Since $S_o = 1 - S_w$, the S_o fields are simply the inverse of S_w. At 0.01 day, the water saturation immediately decreases at the oil leak location, but remains above 0.99 of the initial value at other domain locations. The depression continues to spread out from the center of the oil leak location with time (Figure 10, top). Water saturation after 100 day is below the initial value across the domain, which indicates that NAPL has migrated from the oil leak location throughout the domain, due to viscous, capillary and gravity forces. The variance indicates significant more uncertainty about the location of the NAPL even after a short time. In general, NAPL migrates upward, as the NAPL is less dense than water (Figure 10, bottom). The spill is expected to vary in its vertical and horizontal position significantly as time progresses, due to the heterogeneities in soil properties. At 100 day, although the mean water saturation is smeared around the oil leak area, the variance still presents a radiated distribution around the oil leak location.

[30] The proposed KLME stochastic approach has a high computational efficiency compared to the Monte Carlo method. In the case 1, 200 terms were used for the first order, i.e., the first-order equations (50)–(54) were solved for $P_{o,n}$ and $P_{w,n}$ with n = 1,2,. . .200. Since two-phase flow is a coupled system, solving the linear discretized first-order equations also requires a number of iterations. With the particular solver used, solving the zeroth-order term requires about 20 iterations, whereas the first-order solutions usually converge after 10 iterations each, so the total number of runs for KLME is about $20 + 10 \times 200 = 2020$. Each realization of the Monte Carlo (MC) simulation using FEHM needs about 50 Newton-Raphson iterations, because the parameter fields are not as smooth as in the KLME approach. Thus approximately 100,000 iterations are required for 2,000 MC simulations, which is nearly 50 times the effort required for the KLME approach. The actual run time for KLME is 0.5 hr, while MC simulations require 15 hr on the same computer. Clearly the computational effort would increase significantly if we added the second-order corrections to the first-order KLME results, but the overall simulation time would still be much less than that of MC simulation [*Chen et al.*, 2005].

6. Summary and Conclusions

[31] A stochastic transient two-phase flow numerical model was developed based on Karhunen-Loeve, polynomial expansions and perturbation methods to evaluate, up to first-order accuracy, the pressure moments in randomly heterogeneous subsurface zone. We demonstrated the KLME approach with an example of transient water-oil flow in a two-dimensional rectangular domain and compared the results with those from Monte Carlo simulations. We also provided another example with different conditions, to evaluate the sensitivity of the KLME approach to different flow conditions. The main findings of this paper are summarized as follows.

[32] 1. The KLME method is applicable to stochastic analysis of transient water-oil flow with widely used van Genuchten constitutive relationships instead of the exponential type model. The success of this application makes the current KLME model more acceptable, comparable, and practical.

[33] 2. The comparison of KLME results with Monte Carlo simulations using FEHM indicates that this proposed stochastic approach and the executable numerical model produce very similar results, and the KLME approach is much more efficient than the MC approach. A better match is likely to be obtained if we include second-order terms, with some loss in computational efficiency. However, we don't expect the results to be significantly different.

[34] 3. The transient water-oil two-phase flow is a coupled system, so all the zeroth-, first-order equations need several iterations to converge on a solution. However, the

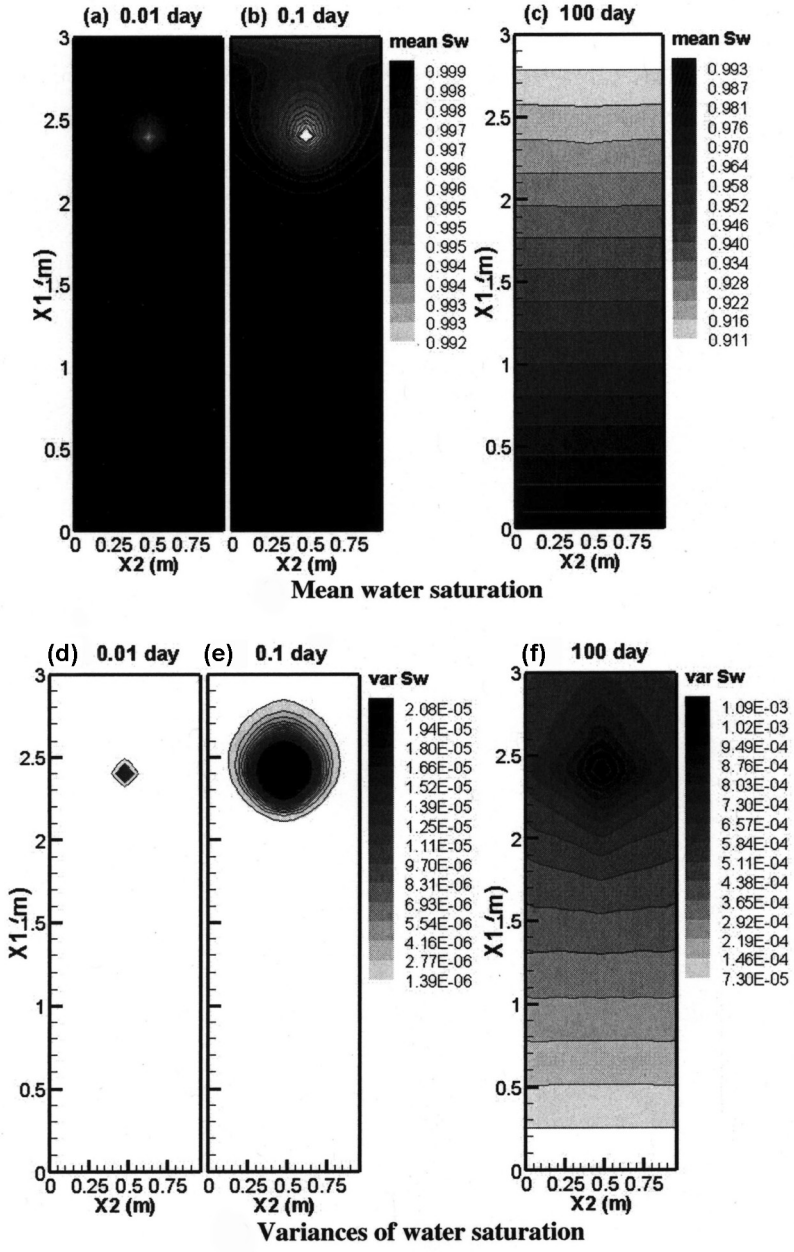

Figure 10. Water saturation (top) mean S_w and (bottom) variance of S_w for case 2 at three time steps: (a and d) 0.01 day, (b and e) 0.1 day, and (c and f) 100 day.

first-order discretized equations are linear and require less iteration than the zeroth-order equations, which are nonlinear. In addition, the left hand coefficient matrix resulting from discretization of the KL-based moment equations is the same for zeroth- and first-order equations. These features make the numerical modeling very efficient because it is not necessary to rebuild the coefficient matrix for different orders of the perturbation equations in every iteration calculation.

[35] 4. The stochastic transient water-oil model is capable of modeling water/oil infiltration at any domain boundary, water/oil leakage at any location of domain and any modeling time, which indicate a potential application not only for remediation analysis, but also for the petroleum industry and other large heterogeneous multiphase systems, where uncertainty analysis requires new approaches to understand the implications of these nonlinear, coupled systems.

[36] **Acknowledgment.** The authors would like to acknowledge funding from the CARE program at Los Alamos National Laboratory, as well as support from the Bren School of Environmental Science and Management at the University of California, Santa Barbara.

References

Abdin, E., and J. Kaluarachchi (1997a), Stochastic analysis of three-phase flow in heterogeneous porous media: 1. Spectral/perturbation approach, *Water Resour. Res.*, *33*(7), 1549–1558.

Abdin, E., and J. Kaluarachchi (1997b), Stochastic analysis of three-phase flow in heterogeneous porous media: 2. Numerical simulations, *Water Resour. Res.*, *33*(7), 1559–1566.

Abriola, L. (1989), Modeling multiphase migration of organic chemicals in groundwater systems—A review and assessment, *Environ. Health Perspect.*, *83*, 117–143.

Abriola, L., and G. Pinder (1985), A multiphase approach to the modeling of porous media contamination by organic compounds: 1. Equation development, *Water Resour. Res.*, *21*(1), 11–18.

Bellin, A., P. Salandin, and A. Rinaldo (1992), Simulation of dispersion in heterogeneous porous formations: Statistics first-order theories, convergence of computations, *Water Resour. Res.*, *28*(9), 2211–2227.

Chang, C., M. Kemblowski, J. Kaluarachchi, and A. Abdin (1995), Stochastic analysis of two-phase flow in porous media: I. Spectral/perturbation approach, *Transp. Porous Media*, *19*, 233–259.

Chen, M., D. Zhang, A. Keller, and Z. Lu (2005), A stochastic analysis of steady state two-phase flow in heterogeneous media, *Water Resour. Res.*, *41*, W01006, doi:10.1029/2004WR003412.

Chin, D., and T. Wang (1992), An investigation of the validity of first-order stochastic dispersion theories in isotropic porous media, *Water Resour. Res.*, *28*(6), 1531–1542.

Chrysikopoulos, C. V., and Y. Sim (1996), One-dimensional virus transport in homogeneous porous media with time dependent distribution coefficient, *J. Hydrol.*, *185*, 199–219.

Chrysikopoulos, C. V., P. K. Kitanidis, and P. V. Roberts (1990), Analysis of one-dimensional solute transport through porous media with spatially variable retardation factor, *Water Resour. Res.*, *26*(3), 437–446.

Courant, R., and D. Hilbert (1953), *Methods of Mathematical Physics*, Wiley-Interscience, Hoboken, N. J.

Dagan, G. (1989), *Flow and Transport in Porous Formations*, Springer, New York.

Delshad, M., G. Pope, and K. Sepehmoori (1996), A compositional simulator for modeling surfactant enhanced aquifer remediation: 1. Formulation, *J. Contam. Hydrol.*, *23*(4), 303–327.

Deutsch, C., and A. Journel (1992), *GSLIB: Geostatistical Software Library*, Oxford Univ. Press, New York.

Gelhar, W. (1993), *Stochastic Subsurface Hydrology*, Prentice-Hall, Upper Saddle River, N. J.

Ghanem, R., and S. Dham (1998), Stochastic finite element analysis for multiphase flow in heterogeneous porous media, *Transp. Porous Media*, *32*, 239–262.

Ghanem, R., and D. Spanos (1991), *Stochastic Finite Elements: A Spectral Approach*, Springer, New York.

Graham, W., and D. McLaughlin (1989), Stochastic analysis of nonstationary subsurface solute transport: 1. Unconditional moments, *Water Resour. Res.*, *25*(2), 215–232.

Karhunen, K. (1947), Uber lineare methoden in der wahrscheinlichkeitsrechnung, *Ann. Acad. Sci. Fennicae, Ser. A*, *37*, 3–79, (Engl. Transl., *Rep. T-131*, RAND Corp., Santa Monica, Calif., 1960.)

Keller, A., and M. Chen (2002), Seasonal variation in bioavailability of residual NAPL in the vadose zone, paper presented at International Groundwater Symposium, Int. Assoc. of Hydrol. Sci., Berkeley, Calif.

Keller, A., and M. Chen (2003), Effect of spreading coefficient on three-phase relative permeability of nonaqueous phase liquid, *Water Resour. Res.*, *39*(10), 1288, doi:10.1029/2003WR002071.

Keller, A., M. Blunt, and P. Roberts (2000), Behavior of dense non-aqueous phase liquids in fractured porous media under two-phase flow conditions, *Transp. Porous Media*, *38*, 189–203.

Loeve, M. (1948), *Fonctions aleatorires du second ordre*, Gauthier, Villars, Paris.

Lu, Z., and D. Zhang (2002), Stochastic analysis of transient flow in heterogeneous, variably saturated porous media: The van Genuchten–Mualem constitutive model, *Vadose Zone J.*, *1*, 137–149.

Lu, Z., and D. Zhang (2004a), Conditional simulations of flow in randomly heterogeneous porous media using a KL-based moment-equation approach, *Adv. Water Resour.*, *27*, 859–874.

Lu, Z., and D. Zhang (2004b), A comparative study on uncertainty quantification for flow in random heterogeneous media using Monte-Carlo simulations, the conventional and KL-based moment equations approach, *SIAM J. Sci. Comput.*, *26*(2), 558–577.

Lu, Z., and D. Zhang (2005), Accurate, efficient quantification of uncertainty for flow in heterogeneous reservoirs using the KLME approach, paper presented at Reservoir Simulation Symposium, Soc. of Pet. Eng., Houston, Tex.

Mercer, W., and M. Cohen (1990), A review of immiscible fluids in the subsurface: Properties, models, characterization and remediation, *J. Contam. Hydrol.*, *6*, 107–163.

Parker, J., and R. Lenhard (1990), Determining three-phase permeability-saturation-pressure relations from two-phase system measurements, *J. Pet. Sci. Eng.*, *4*, 57–65.

Parker, J., J. Zhu, T. Johnson, V. Kremesec, and E. Hockman (1994), Modeling free product migration and recovery at hydrocarbon spill sites, *Groundwater*, *32*, 119–128.

Smith, L., and R. Freeze (1979), Stochastic analysis of steady state groundwater flow in a bounded domain: 2. Two-dimensional simulations, *Water Resour. Res.*, *15*(6), 1543–1559.

Tartakovsky, A. M., P. Meakin, and H. Huang (2004), Stochastic analysis of immiscible displacement of the fluids with arbitrary viscosities and its dependence on support scale of hydrological data, *Adv. Water Resour.*, *27*(12), 1151–1166.

van Genuchten, M. (1980), A closed form solution for predicting the hydraulic conductivity of unsaturated soils, *Soil Sci. Soc. Am. J.*, *44*, 892–898.

Yang, J., D. Zhang, and Z. Lu (2004), Stochastic analysis of saturated-unsaturated flow in heterogeneous media by combing Karhunene-Loeve expansion and perturbation method, *J. Hydrol.*, *29*, 418–438.

Zhang, D. (1998), Numerical solutions to statistical moment equations of groundwater flow in nonstationary, bounded heterogeneous media, *Water Resour. Res.*, *34*(3), 529–538.

Zhang, D. (1999), Non-stationary stochastic analysis of transient unsaturated flow in randomly heterogeneous media, *Water Resour. Res.*, *35*(4), 1127–1141.

Zhang, D. (2002), *Stochastic Methods for Flow in Porous Media: Coping With Uncertainties*, Springer, New York.

Zhang, D., and Z. Lu (2002), Stochastic analysis of flow in a heterogeneous unsaturated-saturated system, *Water Resour. Res.*, *38*(2), 1018, doi:10.1029/2001WR000515.

Zhang, D., and Z. Lu (2004), Evaluation of higher-order moments for saturated flow in randomly heterogeneous media via Karhunen-Loeve decomposition, *J. Comput. Phys.*, *194*(2), 773–794.

Zhang, D., and A. Sun (2000), Stochastic analysis of transient saturated flow through heterogeneous fractured porous media: A double-permeability approach, *Water Resour. Res.*, *36*(4), 865–874.

Zyvoloski, G., B. Robinson, Z. Dash, and L. Trease (1997), Summary of the models and methods for the FEHM applications—A finite-element heat- and mass-transfer code, *Rep. LA-13307-MS*, Los Alamos Natl. Lab., Los Alamos, N. M.

M. Chen and A. A. Keller, Bren School of Environmental Sciences and Management, University of California, 3420 Bren Hall, Santa Barbara, CA 93106-5131, USA. (keller@bren.ucsb.edu)

Z. Lu and G. A. Zyvoloski, Hydrology, Geochemistry, and Geology Group (EES-6), Los Alamos National Laboratory, Los Alamos, NM 87545, USA.

D. Zhang, Mewbourne School of Petroleum and Geological Engineering, University of Oklahoma, Norman, OK 73019, USA.